Eur Biophys J (2004) 33: 572–579
DOI 10.1007/s00249-004-0400-9

ARTICLE

**Jan Sun · Elena E. Pohl · Oxana O. Krylova
Eberhard Krause · Igor I. Agapov
Alexander G. Tonevitsky · Peter Pohl**

Membrane destabilization by ricin

Received: 7 January 2004 / Revised: 24 February 2004 / Accepted: 26 February 2004 / Published online: 26 March 2004

Abstract Ricin is a promising candidate for the treatment of cancer because it can be selectively targeted to tumor cells via linkage to monoclonal antibodies. Biochemical evidence suggests that escape of ricin or its ribosome-inactivating subunit from an intracellular compartment is mediated by retrograde transport to the endoplasmic reticulum and subsequent direction into the ER-associated degradation pathway. Alternatively, lipase activity of ricin may facilitate leakage from endocytic vesicles. We have observed ricin-mediated release of macromolecular dyes from lipid vesicles that mimic the composition of endosomal membranes. Release of small molecules occurs to the same extent, suggesting an all-or-none mechanism due to bilayer destabilization. The level of accompanying membrane fusion depends on vesicle composition. Since it takes 24 h of incubation before the first traces of lysolipids are detectable by matrix-assisted laser desorption/ionization mass spectrometry, membrane destabilization is not due to the lipase activity of ricin.

Abbreviations CF: Carboxyfluorescein · DPhPC: Diphytanoyl-phosphatidylcholine · DPA: Dipicolinic acid · EDTA: Ethylendiamine-tetracetate · ER: Endoplasmic reticulum · ERAD: ER-associated degradation · FRET: Fluorescence-resonance energy transfer · GM_1: Monosialoganglioside · MALDI-MS: Matrix-assisted laser desorption/ionization mass spectrometry · MES: 2-Morpholino-ethanesulfonic acid · NBD-PE: *N*-(7-nitro-2,1,3-benzoxadiazol-4-yl)-phosphatidylethanolamine) · PC: Phosphatidylcholine · PE: Phosphatidylethanolamine · PG: Phosphatidylglycerol · Rh-PE: *N*-(lissamine rhodamine B sulfonyl)-phosphatidylethanolamine · RIP: Ribosome-inactivating protein · RTA: A-chain of ricin · RTB: B-chain of ricin · TES: *N*-[Tris-(hydroxymethyl)-methyl]-2-aminoethansulfonic acid · TOF: Time-of-flight

J. Sun · O. O. Krylova · E. Krause · P. Pohl (✉)
Campus Berlin Buch, Forschungsinstitut für Molekulare Pharmakologie, Robert Roessle Str. 10, 13125 Berlin, Germany
E-mail: pohl@fmp-berlin.de
Tel.: +49-30-94793291
Fax: +49-30-94793283

E. E. Pohl
Neuroscience Research Center, Charite, Humboldt-Universität, Schumannstr. 20/21, 10117 Berlin, Germany

I. I. Agapov · A. G. Tonevitsky
Institute of Transplantology and Artificial Organs, Shchukinskaya St. 1, 123182 Moscow, Russia

P. Pohl
Lehrstuhl für Experimentelle Biophysik, Institut für Biologie, Humboldt-Universität, Invalidenstr. 43, 10115 Berlin, Germany

Introduction

Ricin is a plant toxin from the seeds of *Ricinus communsis* belonging to the ribosome-inactivating proteins (RIP). Structurally, it is a heterodimeric glycoprotein comprising a ribosome-inactivating A-chain (RTA) (Zhang and Wang 1986) and a galactose-binding B-chain (RTB) (Rutenber et al. 1987) covalently linked by a single disulfide bond. Upon RTB binding to glycoproteins and glycolipids on the cell surface, the toxin is taken up by endocytosis (van Deurs et al. 1989). Ricin is internalized by both clathrin-dependent and clathrin-independent mechanisms (Sandvig and van Deurs 1996). A single A-chain molecule can inactivate 1,000–2,000 mammalian cell ribosomes/min under physiological conditions (Sandvig and van Deurs 2000). Due to this extreme cytotoxicity, a therapeutic use seems to be promising in the treatment of cancer (Brinkmann and Pastan 1994; Pennell and Erickson 2002), of autoimmune (Raso 1994), graft-versus-host diseases (Cobbold et al. 1984; Van Oosterhout et al. 2000), and of chronic inflammation (Thepen et al. 2000). Selective targeting of specific cell types is achieved by linking the holotoxin or its A-subunit to antibodies (Brinkmann and Pastan 1994). However, ricin-based immunotoxins are less

cytotoxic than native RIPs (Tonevitsky et al. 1996; Sharma et al. 1999). Also, when RTA-based constructs are administered in vivo, a disappointingly low antitumour efficiency is observed. Most likely, some functional property is discarded with the RTB moiety (Lord et al. 1994).

An interesting hypothesis is that the lipase activity of RTB (Moulin et al. 1994; Morlon-Guyot et al. 2003) may be involved in the enhancement of intoxication by ricin, contributing thereby to the penetration process of the ricin molecule into the target cell (Fu et al. 1996). However, the rather weak activity of the holotoxin on phosphotidylcholines and phosphotidylethanolamines (Helmy et al. 1999) has not yet been proven to cause membrane defects at a physiologically relevant timescale.

A comparison of the cytotoxicities of different members of the RIP family reveals great diversity. For example, the tetramer *Ricinus communis* agglutinin that consists of two A-chains and two B-chains is 2,000-fold less toxic than ricin when injected intraperitoneally into mice (Saltvedt 1976). The difference in the cytotoxicities observed with different lectins does not simply reflect the difference in biological activity of the respective A-chains (Brinkmann and Pastan 1994). Rather, it appears to be due to differences in the protein–lipid interactions which are crucial for the delivery of the A-chains into the cytosol of target cells (Ishida et al. 1983; Hoekstra and Düzgünes 1986; O'Hare et al. 1992). Based on RIP-induced membrane dehydration (Pohl et al. 1998b) and membrane fusion (Utsumi et al. 1989; Pohl et al. 1998a), a model is suggested in which the toxicity of the RIPs is partially determined by their fusogenicity. Herein, fusion is hypothesized to allow the RIPs to leak across endocytic vesicles to permit them access to cytoplasmic ribosomes (Pohl et al. 1998a). However, direct evidence for a ricin-induced release of macromolecules from vesicles is missing.

So far, only RTA-induced release of calcein from vesicles has been observed (Day et al. 2002). Due to RTA–lipid interactions, vesicle destabilization occurred, and most importantly, RTA unfolded. This lipid-mediated unfolding was suggested to be the mechanism by which ricin disguises itself as misfolded protein to be imported into the cytosol by the endoplasmic-reticulum (ER) quality-control system (Hazes and Read 1997; Wesche 2002). Exposed hydrophobic patches should lead to better recognition by the ER-associated-degradation (ERAD) transport machinery. According to circumstantial evidence, the ERAD pathway is involved in the transfer of ricin from the Golgi apparatus to the ER (Simpson et al. 1999; Romisch 1999; Teter and Holmes 2002). This hypothesis agrees well with the finding that a fraction (5%) of the endocytosed ricin is transported to the Golgi apparatus (van Deurs et al. 1986).

Summarizing, the effect of ricin on a membrane may be threefold:

1. Ricin hydrolyzes membrane lipids causing defects in membrane integrity.
2. Ricin causes membrane fusion accompanied by leakage of aqueous content of vesicles.
3. Insertion of hydrophobic ricin domains results in membrane destabilization.

Here, we show that ricin destabilizes lipid vesicles. At the same time, it is unable to fuse endosomal-model membranes or to catalyze lipid hydrolysis to an extent that would account for vesicle destruction and content release.

Materials and methods

Proteins

Ricin and its catalytic subunit RTA were purified from *Ricinus communis* seeds as described in Tonevitsky et al. (1990). To completely remove RTB, preparations of RTA were further purified on Sepharose 4B (Pharmacia, Sweden) with fixed asialofetuin (Sigma). The purity of the preparation was at least 99% (Fig. 1).

Liposomes

Large unilammelar vesicles (LUVs) were prepared by an extrusion technique (MacDonald et al. 1991) using the small-volume apparatus LiposoFast (Avestin Inc., Ottawa, Canada) with filters of 100-nm pore diameter (Nucleopore Filtration Products, Pleasonton, CA). Vesicles with three different lipid compositions were formed. All vesicles contained monosialoganglioside (GM_1) to serve as a lectin receptor. The vesicles were composed of: (1) 97 mol% diphytanoyl-phosphatidylcholine (DPhPC) and 3 mol% GM_1; (2) 97 mol% *Escherichia coli* polar-lipid extract and 3 mol% GM_1; (3) 45 mol% egg phosphatidylcholine (PC), 20 mol% phosphatidylethanolamine (PE), 8 mol% phosphatidylserine (PS), 10 mol% cholesterol, 9 mol % sphingomyelin, 4 mol% phosphoinisotol, 1 mol% cardiolipin, and 3 mol% GM_1 (all Avanti Polar Lipids, Alabaster, AL, USA). The synthetic DPhPC was used for the analysis of lipase activity because it does not contain any traces of lysolipids. The *Escherichia coli* lipid was chosen because the high content of PE is known both to facilitate membrane fusion in general (Chernomordik et al. 1995) and to promote ricin/RTA-induced fusion in particular (Pohl et al. 1998a). The high amount of unsaturated fatty acids ($>50\%$) is also beneficial, because they are

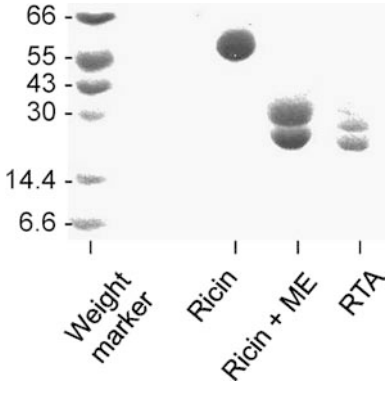

Fig. 1 SDS-PAGE (15%) analysis of ricin and its catalytic (RTA) subunit. *Lane 1* Low weight marker, *lane 2* ricin (without mercaptoethanol), *lane 3* ricin (with mercaptoethanol), *lane 4* two RTA bands which differ in their level of glycosilation. The method of Laemmli was used (Laemmli 1970)

known to ease RIP adsorption. RIP adsorption has been correlated with looser packing of polyunsaturated lipids at the lipid-water interface (Pohl et al. 1998b). According to Avanti Polar Lipids, the highly purified *E. coli* polar-lipid extract is a mixture of 67% PE, 23.2% phosphatidylglycerol (PG), and 9.8% cardiolipin. The third lipid mixture was prepared to mimic the lipid composition of endosomes.

At a final concentration of 25–100 μM, the lipid vesicles were suspended in a buffer solution containing 150 mM NaCl and 10 mM TES. In some of the experiments, a reduction in pH from 7.4 to 6.0 was achieved by adding a small aliquot of a concentrated MES solution (200 mM buffer and 150 mM NaCl). All experiments were performed at 37 °C.

To study the intermixing of the aqueous content of the vesicles (Düzgünes and Wilschut 1993), fluorescence measurements were carried out using a modular spectrofluorimeter (ORIEL Instruments, Stratford, CT, USA) equipped with a thermostated cuvette holder and a magnetic stirrer. The mixing of membrane lipids was shown by fluorescence-resonance energy transfer (FRET) (Hoekstra and Düzgünes 1993).

Fluorescence-resonance energy transfer

Liposomes were labelled with 1 mol% of two fluorescent derivatives of phospholipids, namely *N*-(7-nitro-2,1,3-benzoxadiazol-4-yl)-PE (NBD-PE) and *N*-(lissamine rhodamine B sulfonyl)-PE (Rh-PE) (Hoekstra and Düzgünes 1993). FRET is possible between both dyes, i.e. NBD excitation may result in Rh-PE fluorescence. The labelled LUVs and a fourfold excess of unlabelled vesicles of similar lipid composition were mixed in a fluorescence cuvette at 37 °C and pH 7.4. As the mixed liposomes were allowed to fuse with each other by protein addition, the labels diffused into the membranes of unlabelled liposomes, resulting in a decrease in FRET. The fluorescence obtained after lysing the vesicles with 1% Triton X-100 (Serva, Heidelberg, Germany) was set to 100% after having been corrected for the detergent effect on the quantum yield of *N*-NBD-PE.

Mixing of aqueous contents

Mixing of the aqueous contents of the vesicles was followed by the Tb^{3+}/DPA assay (Düzgünes and Wilschut 1993). A population of Tb^{3+}-containing vesicles and a population of DPA-containing vesicles were mixed in a TES buffer (10 mM TES, 0.1 mM EDTA, and 150 mM NaCl; pH 7.4; 37 °C). Fusion of vesicles was indicated by an increase in the fluorescence intensity at 545 nm, arising due to the excitation at 276 nm from the formation of a highly fluorescent $[Tb(DPA)_3]^{3-}$ chelation complex. A cutoff filter (530 nm) was placed between the sample and the emission monochromator to eliminate interference from light scattering.

The phospholipid vesicles were prepared in (1) 2.5 mM $TbCl_3$, 50 mM sodium citrate, 10 mM TES, and 50 mM NaCl and (2) 50 mM DPA, 70 mM NaCl, and 10 mM TES. They were separated from the nonencapsulated material by gel filtration. PD-10 columns (Supelco, Bellefonte, PA, USA) filled with Sephadex G-25 M were used. The chromatography column was equilibrated with an elution buffer containing 150 mM NaCl, 10 mM TES, and 1 mM EDTA. EDTA prevented Tb^{3+} from binding to the vesicle membrane.

Fusion was monitored in a 100-μM lipid suspension recruited in equal parts from the vesicles trapped with Tb^{3+} and from those containing DPA. The extent, *F*, of fusion was calculated as:

$$F = \frac{I_p - I_0}{I_{100} - I_0} 100\,\% \qquad (1)$$

where I_0, I_p and I_{100} are, respectively, the fluorescence intensities in the absence of the protein, after protein addition and after vesicle solubilization with 0.5% deoxycholic acid (Sigma).

Leakage of vesicle contents

Tb^{3+} release into the medium Leakage of preencapsulated Tb^{3+} was measured by following its chelation with DPA. Measurements were carried out in the same way as the fusion measurements, except that only the population of Tb^{3+} vesicles (at the same total phospholipid concentration as in the corresponding fusion measurements) was used. To eliminate the EDTA in the first buffer, the chromatographed Tb^{3+} vesicles were rechromatographed, but equilibrated with 150 mM NaCl and 10 mM TES. After adding 10 μM free DPA, the buffer was used to monitor leakage. The fluorescence scale was calibrated in the same way as in the corresponding fusion measurements.

Release of carboxyfluorescein Toxin-mediated carboxyfluorescein (CF; Sigma) release was monitored by encapsulating the dye at self-quenching concentration in the phospholipid vesicles (Weinstein et al. 1977; Düzgünes and Wilschut 1993). The vesicles were prepared in 100 mM 5(6)-carboxyfluorescein, 100 mM NaCl, and 10 mM TES. The vesicles were separated from the nonencapsulated material by gel filtration. Release of CF was measured in 150 mM NaCl solution buffered with 10 mM TES. The final lipid concentration was 25 μM. Excitation and emission wavelengths were 490 and 520 nm, respectively. For calibration of the fluorescence scale (F is substituted by $-F$ in Eq. 1), maximum release was induced by 0.1% (v/v) Triton X-100.

Matrix-assisted laser desorption/ionization mass spectrometry

Each preparation of LUVs was divided into two fractions. Ricin was added to the first fraction and an equal amount of buffer to the second. After incubation, the lipid was extracted from both fractions with the Folch mixture (methanol-chloroform, 1:2, v/v). Ricin was discarded along with the water/methanol layer. After evaporation of the solvent, the lipid was dissolved in methanol and mixed with the 2,5-dihydroxybenzoic-acid matrix solution. The latter consisted of 10 mg matrix dissolved in 1 ml of 0.1% trifluoracetic acid in acetonitrile-water (1:1, v/v). One μl of the resulting mixture was applied to the sample plate. Samples were air-dried at room temperature (24 °C). Matrix-assisted laser desorption/ionization mass spectrometry (MALDI-MS) measurements were performed on a Voyager-DE STR BioSpectrometry Workstation MALDI-TOF mass spectrometer (PerSeptive Biosystems, Inc., Framingham, MA, USA) as described in Krause et al. (1999). The reflection mode was used at an acceleration voltage of 20 kV, 70% grid voltage, and a delay of 200 ns. Each spectrum obtained was the mean of 256 laser shots.

Results

Intermixing of membrane lipids

At neutral pH, ricin caused NBD/Rh-labelled vesicles to fuse with unlabelled vesicles as revealed by a small but significant decrease in FRET. Acidification further diminished FRET (Fig. 2). Specific protein binding to a membrane receptor was required as confirmed by the inhibitory effect of galactose. Galactose decreased the level of membrane-lipid intermixing by competing for ricin binding with the membrane-bound GM_1.

Previously, ricin was described to promote membrane fusion that was driven by an osmotic gradient (Pohl et al. 1998a). This result was confirmed by a decrease in FRET observed after the NaCl concentration was in-

creased from 150 to 300 mM. Again, the effect was partially inhibited by galactose (Fig. 2).

The experiments carried out with ricin were repeated with the isolated A-chain. The subunit decreased FRET at both acidic and neutral pH (Fig. 2). An increase in the osmotic pressure enhanced the RTA-induced intermixing of membrane lipids. Addition of galactose was without any effect on FRET because the A-chain does not possess a sugar-binding motif (Fig. 2).

Mixing of aqueous contents

In contrast to its effect on FRET, ricin did not induce aqueous contents mixing at neutral pH (Fig. 3). Only the RTA subunit-mediated vesicle–vesicle fusion as revealed by the fluorescence of the Tb^{3+}/DPA complex (Fig. 3). In an acidic environment, both proteins promoted leakage, the A-chain being more effective than the holoricin. As already found with the lipid-mixing assay, increased osmotic pressure was accompanied by increased vesicle fusion. The holoricin was able to cross-link membranes of two or more vesicles. Upon osmotically induced shrinking, the vesicles experienced mechanical stress leading to fusion. This result agreed well with the reported capability of RTA and ricin to raise the level of constitutive vesicle fusion with planar membranes (Pohl et al. 1998a). The transmembrane osmotic gradients used to drive constitutive fusion (Pohl et al. 1998a) and to release intravesicular dyes (Figs. 2, 3, 4, and 5) were close in magnitude.

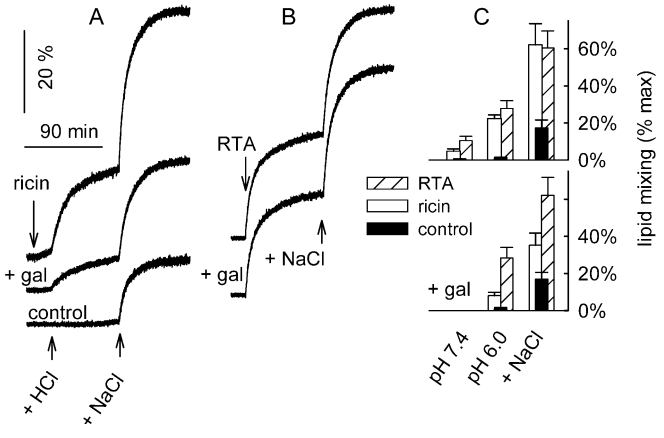

Fig. 2A–C Protein-induced membrane fusion visualized by lipid mixing assay. Fusion of unlabelled vesicles with vesicles bearing Rh and NBD resulted in a decreased efficiency of the resonance energy transfer between both dyes. Representative time courses of relative donor fluorescence (530 nm) and average fluorescence are shown. **A** Ricin-induced lipid mixing. Ricin-induced effects were promoted by a pH decrease from 7.4 to 6.0, and subsequently, by osmotic stress (an increase in the NaCl buffer concentration to 300 mM). The partial inhibition of reduction in FRET by addition of 20 mM galactose demonstrates specific lectin binding to monosialoganglioside (GM_1). **B** RTA-induced membrane fusion. **C** Average fluorescence (at least five experiments for each *bar*) from **A** and **B**

Leakage of vesicle content

Although ricin did not induce aqueous contents mixing at neutral pH, it mediated Tb^{3+} leakage (Fig. 4). The extent of leakage induced by the fusogenic RTA was greater. To show that leakage is specific to membrane-bound ricin, the experiments were repeated in the presence of galactose. The competition of both galactose and the membrane receptor GM_1 for ricin binding decreased the lectin-mediated Tb^{3+} leakage, suggesting that it is the membrane-bound ricin that is responsible for the effect. Because RTA has no affinity for GM_1, leakage

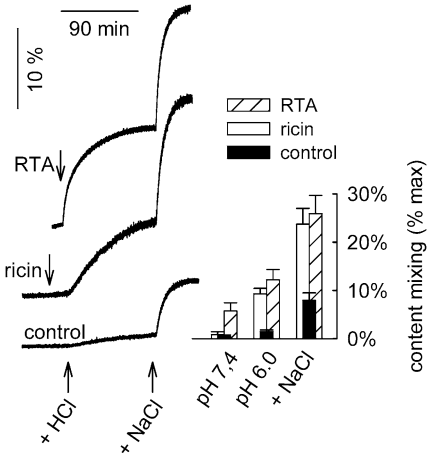

Fig. 3 Ricin- and RTA-induced intermixing of aqueous vesicle content. Two populations of phospholipid vesicles were prepared containing 2.5 mM $TbCl_3$ or 50 mM DPA, respectively. Fusion between them was indicated by the formation of a highly fluorescent $[Tb(DPA)_3]^{3-}$ chelation complex. Representative time courses of fluorescence (*left*) are shown as well as the average fluorescence of at least five repeats (*right*). Vesicle fusion was first monitored at pH 7.4 and subsequently at pH 6.0

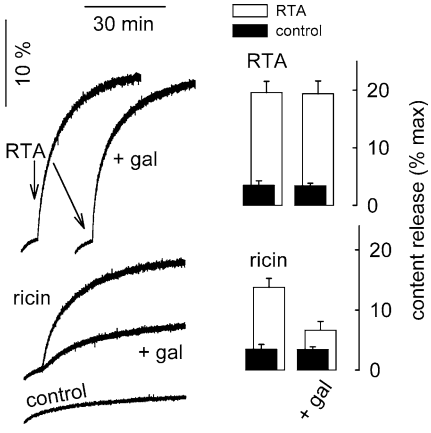

Fig. 4 Ricin- and RTA-induced Tb^{3+} release. Time drive (*left*) and stationary average (*right*) of fluorescence intensity of the $[Tb(DPA)_3]^{3-}$ chelation complex formed in the extravesicular space are shown in percent of the fluorescence intensity measured after vesicle destruction by detergence. Protein and lipid concentrations were 2 and 100 μM, respectively

induced by RTA was found to be independent of the presence of galactose in the medium.

Kinetics of leakage

To gain some insight into the mechanism of protein-lipid interaction, the initial rates, v_i, of lipid mixing, aqueous contents mixing, and release (Pecheur et al. 1997) were compared. The first derivative (at time $t = 0$, the onset of fluorescence increase) of an uniexponential function fitted to the fluorescence tracing (Pecheur et al. 1997) was used to obtain v_i. Lipid and aqueous contents mixing revealed different values for v_i (Fig. 5). Most probably, the extent of fusion was underestimated when registered by contents mixing due to Tb^{3+} leakage. To test this hypothesis, the fluorescence intensity F, measured in the Tb/DPA assay, was corrected for the leakage of aqueous content and dissociation of the Tb/DPA complex:

$$I = F + 0.5Q \quad (2)$$

where I and Q are the corrected fluorescence intensity and the percentage of fluorescence quenching obtained with the Tb/DPA vesicles, respectively. Equation (2) may be used in the early stages of fusion in a 1:1 population of Tb vesicles and DPA vesicles (Düzgünes and Wilschut 1993). As illustrated in Fig. 5, the initial rates of RTA-induced fusion were similar when measured by lipid-mixing and vesicle content mixing assays.

In contrast to RTA, ricin did not induce aqueous content mixing at pH 7.4. The FRET reduction found at the same time suggested vesicle destabilization. Release of aqueous content confirmed this hypothesis (Fig. 5). In an acidic environment, ricin mediated aqueous content mixing. However, lipid mixing was much faster (Fig. 5), suggesting that, at low pH, both fusion and lysis of vesicles took place.

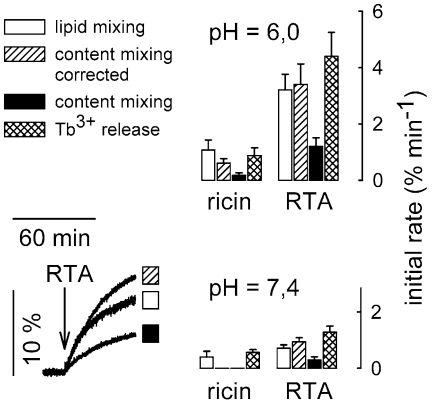

Fig. 5 Comparison of the kinetics of lipid mixing, vesicle contents mixing and Tb^{3+} release. Aqueous content mixing has been corrected for Tb^{3+} release. A representative set of curves (*lower left*) demonstrating the correction procedure according to Eq. (2) is given for RTA-induced fusion. The time constants (*right*) were derived from a monoexponential fit of the respective time courses. In all experiments used for the analysis, protein and lipid concentrations were 2 and 100 μM, respectively

Leakage from vesicles of different lipid composition

To show that aqueous contents release does not result from specific interactions of ricin with *E. coli* lipids, the vesicle composition was varied. Ricin-induced release was observed both from vesicles made from the synthetic lipids DPhPC/GM_1 (Fig. 6A) and from vesicles mimicking the composition of endosomes (Fig. 6B, C). At 0.1% min^{-1}, the initial rate of carboxyfluorescein release from DPhPC/GM_1 vesicles (Fig. 6A) was an order of magnitude smaller than carboxyfluorescein release from *E. coli*/GM_1 vesicles (1.13% min^{-1}). It was comparable to the rate of Tb^{3+} release (0.17% min^{-1}) from endosomal vesicles (Fig. 6B). Equal efficiency of 70 kDa dextran and Tb^{3+} release (Fig. 6C) suggests an all-or-none mechanism of action, i.e. ricin lyses a small population of vesicles when interacting with endosomal lipids. Acidification of the external solution did not alter the amount of lysed vesicles significantly.

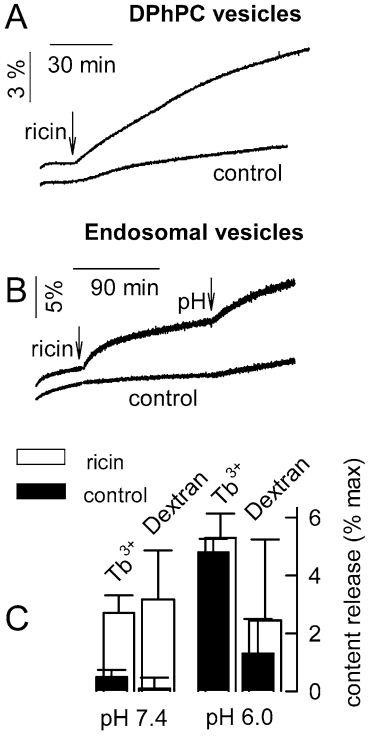

Fig. 6A–C Ricin-induced aqueous content release. **A** Time course of CF fluorescence. Due to its presence in self-quenching concentrations, CF fluorescence is detected after release from DPhPC/GM_1 vesicles. **B** Time course of Tb^{3+} release from vesicles mimicking the composition of endosomal vesicles, with GM_1. The fluorescence of the $[Tb(DPA)_3]^{3-}$ chelation complex formed in the extravesicular space indicates that Tb^{3+} release is comparable to the level of CF release from DPhPC/GM_1 vesicles. For **A** and **B,** fluorescence is measured as percent of the fluorescence intensity after vesicle destruction by detergent. **C** Equal efficiency of 70 kDa dextran and Tb^{3+} release suggests an all-or-none mechanism of action

Visualization of lipolysis by MALDI-TOF-MS

Mass spectrometry of *E. coli* and endosomal-lipid mixtures revealed traces of lysolipids (not shown). Therefore, the analysis of ricin-lipase activity was restricted to DPhPC vesicles (containing 3 mol % GM_1) that were free from lysolipids even after having been incubated for 48 h in buffer solution (Fig. 7). Incubating a suspension of liposomes (lipid concentration, 120 μM) for 12 h with 6 μM ricin did not result in a measurable change in mass distribution. Only after 24 h did the first traces of lipid hydrolysis appear. Accumulation of reaction products during 48 h of incubation resulted in peaks at m/z 552.2 and 553.2 corresponding to the ^{12}C and ^{13}C isotopes of lyso-phytanoyl PC. The intensities of the peaks were comparable to peaks measured after the insertion of 2% lyso-palmitoyl PC into the DPhPC/GM_1 vesicles (Fig. 7). Because ricin-induced vesicle fusion and lyses (Figs. 2, 3, 4, 5 and 6) preceded the occurrence of lysolipids (minutes versus hours), it was concluded that lipase activity does not contribute to vesicle content release.

Discussion

Both ricin and RTA are able to induce leakage of material trapped in vesicular lipid bilayers. Partial, or graded, leakage of vesicle contents has been excluded by the observation that small molecules are released as well as macromolecules. The all-or-none manner of release indicates membrane destabilization. The phospholipase activity of ricin (Moulin et al. 1994; Helmy et al. 1999; Helmy and Pieroni 2000; Lombard et al. 2001) is too weak to destabilize the lipid bilayer at a reasonable timescale. As revealed by MALDI-TOF, measurable quantities of lysolipids appear after 24 h. In contrast, it takes ricin less than 2 h to release intravesicular dyes (Fig. 7), or if administered to cells, to reduce the rate of protein synthesis by one order of magnitude (Casellas et al. 1984). This observation is a strong argument against the hypothesis that the lipase activity of ricin contributes to the penetration process of the ricin molecule inside the target cell (Fu et al. 1996). It is more likely that the unfolding of ricin or its RTA subunit that occurs as the result of membrane binding is the mechanism that enables the toxin to be recognized by the ERAD machinery. Ricin and RTA are speculated to gain access to cytoplasmic ribosomes after retrograde transport by mimicking a misfolded protein (Day et al. 2002).

Unfolding is induced by the hydrophobic effect as well as by electrostatic effects arising from differences in the dielectric constants of the water and the membrane that are related to the partitioning of *H*-bonded peptide bonds (for review see White and Wimley 1999). Both ricin and RTA are able to amplify these effects by dehydrating the bilayer (Pohl et al. 1998b). The major

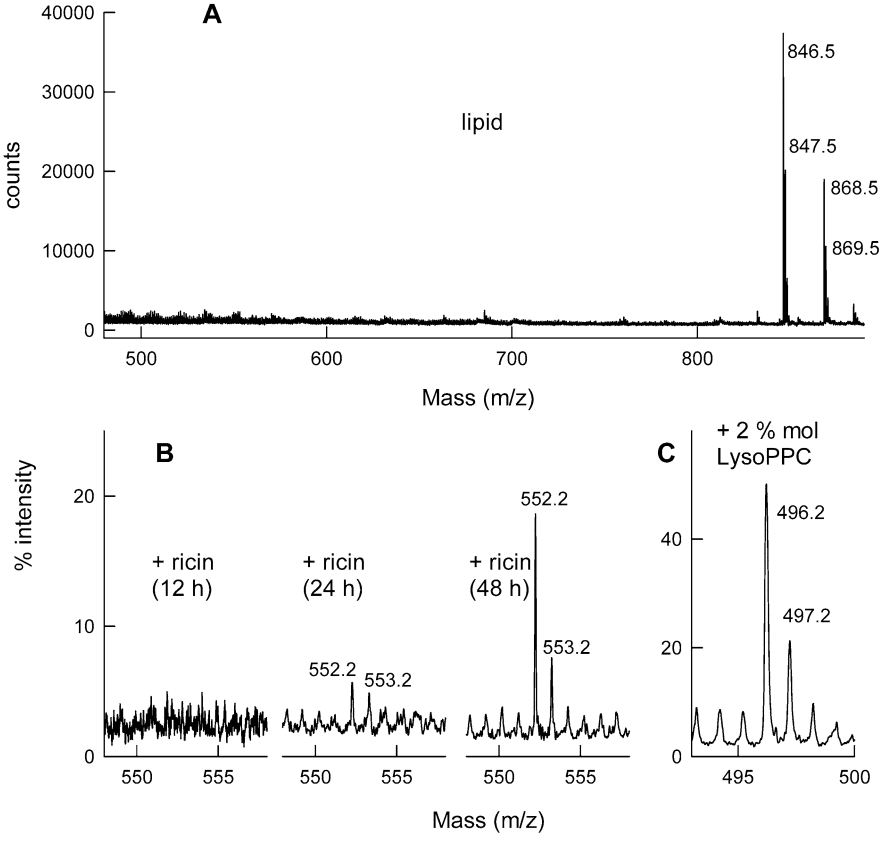

Fig. 7A–C Time scale of ricin-induced lipolysis. **A** MALDI-MS of Folch extracts obtained from DPhPC vesicles (containing 3 mol% GM_1) that have been incubated for 48 h in buffer solution (10 mM TES, 150 mM NaCl, pH 7.4). The *two pairs of peaks* can be assigned to DPhPC (m/z 846.5), its Na adduct (m/z 868.5) and their ^{13}C isotopes (m/z 847.5 and 869.5, respectively). **B** Incubating a suspension of liposomes (lipid concentration 120 μM) with 6 μM ricin for 24 and 48 h resulted in the appearance of *peaks* at m/z 552.2 and 553.2 corresponding to the ^{12}C and ^{13}C isotopes of lyso-phytanoyl PC. An incubation period of 12 h was not sufficient to produce these changes. **C** Addition of 2% lyso-palmitoyl PC to DPhPC/GM_1 vesicles resulted in *two large peaks* at m/z 496.2 and 497.2 corresponding to the lysolipid and its ^{13}C isotope. It was concluded that Folch extraction does not lead to an underrepresentation of lysolipids by mass spectrometry

conformational change of the proteins as they are bound or inserted into the bilayer should lead to an asymmetrical membrane-leaflet extension. The accompanying increases in tension result in defect formation, and depending on membrane composition, in membrane fusion and/or destabilization. Thus, membrane disruption observed in the case of model endosomal membranes (Fig. 6) may arise as a side effect of the ERAD pathway.

The disruption of endosomal membranes is unlikely to be very significant as an alternative mechanism for the translocation of ricin across an intracellular membrane barrier (Pohl et al. 1998a; Pohl et al. 1998b) because:

1. The amount of toxin required to observe intravesicular dye release is higher than physiological levels. Although cluster formation of ricin receptors (Peters et al. 1984a, b) tends to enhance local concentrations of membrane-bound ricin, it is questionable whether micromolar concentrations are reached in vivo.
2. The cytotoxicity of ricin is inhibited when its retrotranslocation by disrupting Golgi stacks is blocked using brefeldin A (Yoshida et al. 1991). If direct-membrane disruption were a significant mechanism, brefeldin A would only partly protect cells against ricin intoxication.
3. ERAD mutations protect against ricin intoxication (Teter and Holmes 2002). They would be ineffective if ricin were delivered from an endosomal compartment.

RTA does not show the specificity of ricin, which interacts only with vesicles presenting galactose residues on their surface. Our observation agrees well with the recent finding that RTA is able to destabilize lipid bilayers in the absence of a membrane receptor (Day et al. 2002). The nonspecific action of RTA may be due to changes in the accessible hydrophobic surface, which result from discharging the B subunit. Thus, the difference between the heterodimeric ricin and its RTA subunit results from the requirement for a membrane receptor (GM_1) and not from the weak lipase activity of the RTB subunit. Qualitatively, ricin and RTA exhibit the same liposome-destabilizing activity provided a membrane receptor is reconstituted into the model membranes.

Because neither its weak fusogenic nor lipolytic activities are responsible for the escape of ricin from endosomal vesicles, membrane destabilization seems to be the only mechanism that remains for cell intoxication. It may well be a side effect of ricin–membrane interaction in the course of which the toxin disguises itself as a misfolded protein thereby subverting the ER-associated protein-degradation pathway to enter target cells (Hazes and Read 1997). The differences in the cytotoxicities observed between ricin-based immunotoxins and the native holotoxin may be due to differences in the protein–lipid interaction when it is altered through the substitution or modification of the B-subunit.

Acknowledgements The work was supported by the Deutsche Forschungsgemeinschaft (Po 533/1–2; Po 533/7–1).

References

Brinkmann U, Pastan I (1994) Immunotoxins against cancer. Biochim Biophys Acta 1198:27–45

Casellas P, Bourrie BJ, Gros P, Jansen FK (1984) Kinetics of cytotoxicity induced by immunotoxins. Enhancement by lysosomotropic amines and carboxylic ionophores. J Biol Chem 259:9359–9364

Chernomordik LV, Kozlov MM, Zimmerberg J (1995) Lipids in biological membrane fusion. J Membr Biol 146:1-14

Cobbold SP, Jayasuriya A, Nash A, Prospero TD, Waldmann H (1984) Therapy with monoclonal antibodies by elimination of T-cell subsets in vivo. Nature 312:548–551

Day PJ, Pinheiro TJT, Roberts LM, Lord JM (2002) Binding of ricin A-chain to negatively charged phospholipid vesicles leads to protein structural changes and destabilizes the lipid bilayer. Biochemistry 41:2836–2843

Düzgünes N, Wilschut J (1993) Fusion assays monitoring intermixing of aqueous contents. Methods Enzymol 3–14

Fu T, Burbage C, Tagge EP, Brothers T, Willingham MC, Frankel AE (1996) Ricin toxin contains three lectin sites which contribute to its in vivo toxicity. Int J Immunopharmacol 18:685–692

Hazes B, Read RJ (1997) Accumulating evidence suggests that several AB-toxins subvert the endoplasmic reticulum-associated protein degradation pathway to enter target cells. Biochemistry 36:11051–11054

Helmy M, Pieroni G (2000) RCA(60): purification and characterization of ricin D isoforms from *Ricinus sanguineus*. J Plant Physiol 156:477–482

Helmy M, Lombard S, Pieroni G (1999) Ricin RGA(60): evidence of its phospholipase activity. Biochem Biophys Res Commun 258:252–255

Hoekstra D, Düzgünes N (1986) *Ricinus communis* agglutinin-mediated agglutination and fusion of glycolipid-containing phospholipid vesicles: effect of carbohydrate head group size, calcium ions, and spermine. Biochemistry 25:1321–1330

Hoekstra D, Düzgünes N (1993) Lipid mixing assays to determine fusion in liposome systems. Methods Enzymol 220:15–32

Ishida B, Cawley DB, Reue K, Wisnieski J (1983) Lipid-protein interactions during ricin toxin insertion into membranes. J Biol Chem 258:5933–5937

Krause E, Wenschuh H, Jungblut PR (1999) The dominance of arginine-containing peptides in MALDI-derived tryptic mass fingerprints of proteins. Anal Chem 71:4160–4165

Laemmli UK (1970) Cleavage of structural proteins during the assembly of the head of bacteriophage T4. Nature 227:680–685

Lombard S, Helmy ME, Pieroni G (2001) Lipolytic activity of ricin from *Ricinus sanguineus* and *Ricinus communis* on neutral lipids. Biochem J 358:773–781

Lord JM, Roberts LM, Robertus JD (1994) Ricin: structure, mode of action, and some current applications. FASEB J 8:201–208

MacDonald RC, MacDonald RI, Menco BPhM, Takeshita K, Subbarao NK, Hu LR (1991) Small-volume extrusion apparatus for preparation of large, unilammellar vesicles. Biochim Biophys Acta 1061:297–303

Morlon-Guyot J, Helmy M, Lombard-Frasca S, Pignol D, Pieroni G, Beaumelle B (2003) Identification of the ricin lipase site and implication in cytotoxicity. J Biol Chem 278:17006

Moulin A, Teissere M, Bernard C, Pieroni G (1994) Lipases of the Euphorbiaceae family: purification of a lipase from *Euphorbia characias* latex and structure-function relationships with the B chain of ricin. Proc Natl Acad Sci USA 91:11328–11332

O'Hare M, Roberts LM, Lord JM (1992) Biological activity of recombinant *Ricinus communis* agglutinin a chain produced in *Escherichia coli*. FEBS Lett 299:209–212

Pecheur EI, Hoekstra D, Sainte-Marie J, Maurin L, Bienvenue A, Philippot JR (1997) Membrane anchorage brings about fusogenic properties in a short synthetic peptide. Biochemistry 36:3773–3781

Pennell CA, Erickson HA (2002) Designing immunotoxins for cancer therapy. Immunologic Res 25:177–191

Peters MW, Barber KR, Grant CW (1984a) Lateral distribution of gangliosides in bilayer membranes: lipid and ionic effects. J Neurosci Res 12:343–353

Peters MW, Mehlhorn IE, Barber KR, Grant CW (1984b) Evidence of a distribution difference between two gangliosides in bilayer membranes. Biochim Biophys Acta 778:419–428

Pohl P, Antonenko YN, Evtodienko VY, Pohl EE, Saparov SM, Agapov II, Tonevitsky AG (1998a) Membrane fusion mediated by ricin and viscumin. Biochim Biophys Acta 1371:11–16

Pohl P, Saparov SM, Pohl EE, Evtodienko VY, Agapov II, Tonevitsky AG (1998b) Dehydration of model membranes induced by lectins from *Ricinus communis* and *Viscum album*. Biophys J 75:2868–2876

Raso V (1994) Review: immunotargeting intracellular compartments. Anal Biochem 222:297–304

Romisch K (1999) Surfing the Sec61 channel: bidirectional protein translocation across the ER membrane. J Cell Sci 112:4185–4191

Rutenber E, Ready M, Robertus JD (1987) Structure and evolution of ricin B chain. Nature 326:624–626

Saltvedt E (1976) Structure and toxicity of pure ricinus agglutinin. Biochim Biophys Acta 451:536

Sandvig K, van Deurs B (1996) Endocytosis, intracellular transport, and cytotoxic action of shiga toxin and ricin. Physiol Rev 76:949–966

Sandvig K, van Deurs B (2000) Entry of ricin and shiga toxin into cells: molecular mechanisms and medical perspectives. EMBO J 19:5943–5950

Sharma S, Podder SK, Karande AA (1999) Comparative studies on kinetics of inhibition of protein synthesis in intact cells by ricin and conjugate of ricin B-chain with momordin. Mol Cell Biochem 200:133–141

Simpson JC, Roberts LM, Romisch K, Davey J, Wolf DH, Lord JM (1999) Ricin A chain utilises the endoplasmic reticulum-associated protein degradation pathway to enter the cytosol of yeast. FEBS Lett 459:80–84

Teter K, Holmes RK (2002) Inhibition of endoplasmic reticulum-associated degradation in cho cells resistant to cholera toxin, *Pseudomonas aeruginosa* exotoxin a, and ricin. Infect Immun 70:6172–6179

Thepen T, van Vuuren AJH, Kiekens RCM, Damen CA, Vooijs WC, van de Winkel JGJ (2000) Resolution of cutaneous inflammation after local elimination of macrophages. Nat Biotechnol 18:48–51

Tonevitsky AG, Zhukova OS, Mirimanova NV, Omylyanenko VG, Timofeeva NV, Bergelson LD (1990) Effect of gangliosides on binding, internalization and cytotoxic activity of ricin. FEBS Lett 264:249–252

Tonevitsky AG, Agapov II, Shamshiev AT, Temyakov DE, Pohl P, Kirpichnikov MP (1996) Immunotoxins containing A-chain of mistletoe lectin I are more active than immunotoxins with ricin A-chain. FEBS Lett 392:166–168

Utsumi T, Ide A, Funatsu G (1989) Ricin A-chain induces fusion of small unilamellar vesicles at neutral pH. FEBS Lett 242:255–258

van Deurs B, Tonnessen TI, Petersen OW, Sandvig K, Olsnes S (1986) Routing of internalized ricin and ricin conjugates to the Golgi complex. J Cell Biol 102:37–47

van Deurs B, Petersen OW, Olsnes S, Sandvig K (1989) The ways of endocytosis. Int Rev Cytol 117:131–177

van Oosterhout YV, van Emst L, Schattenberg AV, Tax WJ, Ruiter DJ, Spits H, Nagengast FM, Masereeuw R, Evers S, De Witte T, Preijers FW (2000) A combination of anti-CD3 and anti-CD7 ricin A-immunotoxins for the in vivo treatment of acute graft versus host disease. Blood 95:3693–3701

Weinstein JN, Yoshikami S, Henkart P, Blumenthal R, Hagins WA (1977) Liposome-cell interaction: transfer and intracellular release of a trapped fluorescent marker. Science 195:489–492

Wesche J (2002) Retrograde transport of ricin. Int J Med Microbiol 291:517–521

White SH, Wimley WC (1999) Membrane protein folding and stability: physical principles. Annu Rev Biophys Biomol Struct 28:319–365

Yoshida T, Chen CC, Zhang MS, Wu HC (1991) Disruption of the golgi apparatus by brefeldin a inhibits the cytotoxicity of ricin, modeccin, and pseudomonas toxin. Exp Cell Res 192:389–395

Zhang XJ, Wang JH (1986) Homology of trichosanthin and ricin A chain. Nature 321:477–478